Thermal Regime and Thermal Properties of Dry Valley Antarctic Permafrost

Daniel Pringle, Warren Dickinson, Joe Trodahl, Alex Pyne. School of Chemical and Physical Sciences, and Antarctic Research Centre

Victoria University of Wellington, Wellington New Zealand (warren.dickinson@vuw.ac.nz pringldani@student.vuw.ac.nz)

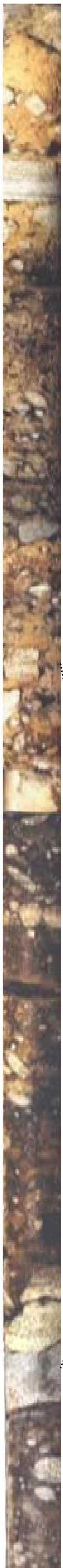

Disordered, unstratified ice/dolerite debris diamict

Ice lens

2m

TM1 Core

Surface layer removed to reveal the undulating ice-horizon (on right).

Installation of thermal array (thin metal tube). Surface debris was then restored to original state.

Site TM1 instrumentation. The array is buried 2m to the right. The blue box houses batteries.

Introduction

The Dry Valleys in East Antarctica are among the driest and coldest environments on Earth. Scientific interest in the area has been increased recently due to the controversial dating of 8.1 Ma ice in Beacon Valley [*Sugden et al*. 1995] and identifying the region as the best analogue of Martian conditions. Average ground temperatures are around -20°C, precipitation is limited to less than 10mm of fine 'diamond dust' snow, and strong katabatic winds prevail. In non-glaciated areas, sand-wedge polygonal ground is ubiquitous [*Sletten et al*, 2003]. The top 10-100cm is typically an ice-free debris layer overlying ice-cemented ground, or buried ice depending on location.

We present comprehensive measurements of the ground temperatures and calculations of the thermal properties (apparent thermal diffusivity, thermal conductivity and heat capacity) of the top 2m of the ice-cemented permafrost, at Table Mountain. In this poster we present an overview of the project and focus on the thermal properties of the ground; in a recent paper [*Pringle et al*, 2003] we also present a comparison of time-series methods for analysing our data and provide details of our new analysis method, outlined below.

Sites and Instrumentation

Two identical, 2 meter long custom-built thermistor arrays [*Trodahl et al*, 2000] were installed in drill holes at sites separated by 100m (Fig. 1). The recovered cores are shown below. Temperatures were read with a precision of better than 0.01°C at 13.5cm spacings every 4 hours from Dec 2000 – Nov 2002, and every 2 hours in ongoing measurements. Site TM1 is in typical local ground with ~5m diameter polygons. TM2 is within a debris flow of unknown age or flow mechanism with ~ 15m diameter polygons. We sought to quantify the thermal regime as much as possible, and were particularly interested in identifying any difference in the thermal properties of the ground between the sites given the factor of 3 difference in polygon scale.

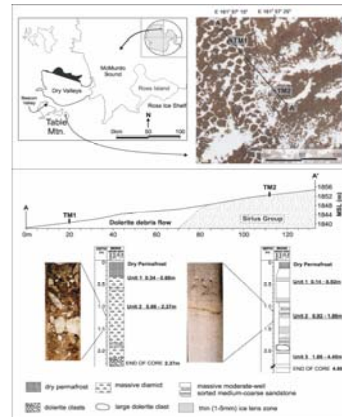

Figure 1. Locations, surface features, and core log of sites TM1 and TM2, Table Mountain. The aerial photo (top right) shows the different scale polygons, demarcated by snow, and the debris flow (left of photo). The middle figure shows the contact between the intrusive Dolerite flow and Sirius. The core stratigraphy and photos from central sections of the cores illustrate the very different compositions at the two sites (detailed in text).

0.7 m

ice lenses

1 m

Sirius sandstone unit

1.4m

ice lenses

2m

TM2 Core

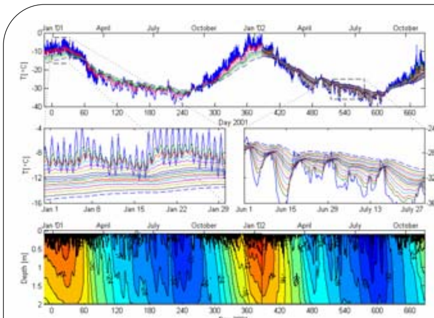

Figure 2. Temperature data and reconstructed temperature field at site TM2. Top plots show T(t) traces for each thermistor. The bottom thermistor (z = 1.98 m) is the dashed line; top thermistor (z = 0.09 m, in surface debris) has the largest amplitude. Only every second thermistor is shown in the top figure.

Analysis: From T(z,t) to Apparent Thermal Diffusivity: D(z,t)

Due to the prevailing cold temperatures the thermal regime is simple: there is no active layer at the surface, only small amounts of trickling snow-melt from direct solar heating of the surface, and no 'zero-curtain' effect. Surface forcing is dominated by the yearly cycle, solar cycling in the summer, and storm cycles in the winter (Fig. 2).

We analysed our temperature data assuming 1-D conductive heat flow, and no latent heat effects. In this case the governing heat equation is:

$$C\frac{\partial T(z,t)}{\partial t} = \frac{\partial k}{\partial z}\frac{\partial T}{\partial z} + k\frac{\partial^2 T}{\partial z^2}, \qquad (1)$$

where C is the volumetric heat capacity and k the thermal conductivity. We have used a graphical finite difference time-series method which returns the mean apparent thermal diffusivity, D=k/C, between successive thermistors. We assume a *locally constant* k and C and to each 3-thermistor region apply the simplified 1-D heat equation:

$$\frac{\partial T(z,t)}{\partial t} = D\frac{\partial^2 T}{\partial z^2}. \qquad (2)$$

The derivatives in equation (2) are estimated directly from our data using finite difference approximations, and the mean apparent thermal diffusivity D determined as the slope of a scatter plot of $\partial T/\partial t$ vs. $\partial^2 T/\partial z^2$ (Fig. 4). Due to errors in both variables, the best-fit gradient is calculated as the geometric mean of the least-squares slopes of $\partial T/\partial t$ vs. $\partial^2 T/\partial z^2$ (blue line) and $\partial^2 T/\partial z^2$ vs. $\partial T/\partial t$ (green line). This is the average apparent thermal diffusivity between the 3 thermistors used to estimate $\partial^2 T/\partial z^2$. By using data from three successive depths, and over different time intervals, we resolve depth- and seasonal- variations in the mean ATD, shown below. (For details, and a comparison with other time-series analysis methods using both equations (1,2) in *Pringle et al.*, 2003).

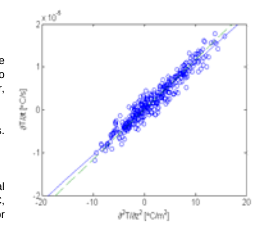

Fig. 3. Graph of $\partial T/\partial t$ vs. $\partial^2 T/\partial z^2$ for data analysis – see text.

Fig. 4. Seasonal variation in apparent thermal diffusivity.

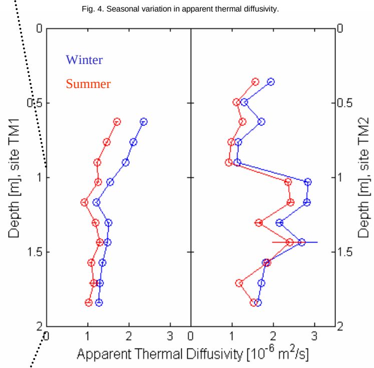

Seasonal Variation in Thermal Diffusivity

We resolved a seasonal variation in the apparent thermal diffusivity profiles at both sites. The ATD was on average 18±9 % higher in the winter than in the summer, consistent with the expected temperature dependence of 11±3% calculated from the expected temperature dependence of the heat capacity and conductivity of the ground components [*Pringle et al*, 2003].

Heat Capacity and Thermal Conductivity

From measured ice fractions (top scale, Fig. 5) and tabulated heat capacities we estimated C(z) profiles in the range 1.75±0.15 MJ/m³°C. The apparent thermal conductivity profiles k(z) =D(z)C(z) are shown in Fig. 5, bottom scale.

The conductivity is generally in the range k=2.5±0.5 W/°Cm, similar to k_{ice}(-20°C) ~ 2.4 W/°Cm and typical mineral components, k_{ice}(-20°C) ~ 3.1 W/°Cm. Our values agree with the single spot measurement of McKay et al (1998) who obtained k=2.5±0.5 W/°Cm for the top 30 cm of the ice cement at nearby Lineaus Terrace. *Our results suggest that this value is a good representation of average thermal properties in the area.*

Site TM1 shows a lower conductivity than TM2 due to higher ice fractions and a more disordered composition (see Fig. 5, Fig. 2 and core images). The region of higher conductivity at site TM2 corresponds to a band of quartose Sirius sandstone which is a laterally extended feature at this location truncated by the debris flow at site TM1. The values in this region are consistent with such a high-quartz content sandstone.

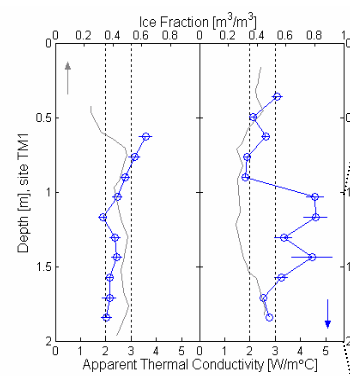

Fig. 5. Apparent thermal conductivity (bottom scale) and ice volume fraction (top scale).

Conclusions

We have determined profiles of the apparent thermal diffusivity, heat capacity and apparent thermal conductivity in the top 2 meters of ice-cemented permafrost at two sites at Table Mountain in the Dry Valleys region. This is the first thorough study of the ground thermal regime and properties of Antarctic permafrost. Due to the low prevailing temperatures and exceedingly low precipitation the system is simple with only conductive heat flow expected.

Using a new graphical finite difference analysis method we resolve ATD profiles which show:

- an abrupt two-fold increase over a sharp compositional boundary at one site,
- a seasonal variation, with wintertime values on average 18±9% higher than summertime values, consistent with the expected underlying temperature dependence.

From core composition we estimate heat capacities in the range 1.75±0.15 MJ/°Cm³. Thermal conductivity profiles k(z)=D(z)C(z) give a typical conductivity of 2.5±0.5 W/°Cm, consistent with ice and typical mineral components at low temperatures. A quartose Sirius sandstone unit at one site has a higher conductivity of 4.1±0.4 W/°Cm, which is consistent with its high quartz content.

It is unlikely that variations in thermal proeprties were important in easblishing 3-fold difference in polygon size at these two sites. We speculate that material characteristics at site TM1 at the time of the debris flow and polygon development were likely to have been more critical.

Acknowledgments

This work was funded by the New Zealand Public Good Science Fund (PGSF). We are very gratefully to Tim Kerr (Scott Base Science Technician), Alan Rennie and Eric Broughton for instrumentation, Mark McGuinness and Juila Boike for helpful discussions, and Webster's Drilling Co. Logistics support was provided by Antarctica New Zealand.

References

McKay, C.P, M.T. Mellon, E.I. Friedmann, Soil Temperatures and stability of ice-cemented ground in the McMurdoDry Valleys, Antarctica, *Antarctic Science*, 10(1), 31-38, 1998.

Pringle D.J., W.W. Dickinson, H.J. Trodahl, A.R. Pyne, 'Depth and Seasonal variations in the thermal properties of Antarctic Dry Valley Permafrost from Temperature Time Series Analysis', in press, *J. Geophys. Res*, doi: 10.1029/2002JB002364.

Sletten, R.S, B. Hallet, R.C. Fletcher, Resurfacing time of terrestrial surfaces by the formation and maturation of polygonal patterned ground, *J.Geophys. Res.* 108 (E4), doi:10.1029/2002JE001914, 2003.

Trodahl, H.J, M.J. McGuinness, P.J. Langhorne, K. Collins, A.E. Pantoja, I.J. Smith, I.J., and T.G. Haskell, Heat transport in McMurdo Sound first-year fast ice, *J. Geophys. Res.*, 150, C5, 11,347-11,358, 2000.

Sugden, D.E., D.R. Marchant, N. J. Potter, R.A. Souchez, G.H. Denton, C.C. Swisher, and J-L. Tison, Preservation of Miocene glacier ice in East Antarctica., *Nature*, 376, 412-414, 1995